Journal of Iranian Dental Association (JIDA)

Original Article

Effect of Selenium Nanoparticles on Streptococcus Mutans Biofilm Gene Expression Using Real Time PCR

Niyousha Noorullahi[1], Farid Abbasi[2], Aliyeh Sehatpour[3] *, Ronak Bakhtiari[4]

[1] Postgraduate Student, Department of Pediatric Dentistry, Faculty of Dentistry, Dental Branch, Islamic Azad University, Tehran, Iran
[2] Associate Professor, Department of Oral Medicine, School of Dentistry, Shahed University, Tehran, Iran
[3] Assistant Professor, Department of Oral Medicine, School of Dentistry, Shahed University, Tehran, Iran
[4] Associate Professor of Biochemistry, Department of Pathobiology, School of Public Health
Tehran University of Medical Sciences, Tehran, Iran

* Corresponding Author: Aliyeh Sehatpour, Email: a.sehhat@shahed.ac.ir
DOI: 10.34172/jida.2303

Abstract

Background: Streptococcus mutans is one of the main causes of dental caries. Although several nanoparticles have been investigated as antimicrobial agents, the antibiofilm potential and mechanistic action of biosynthesized selenium nanoparticles (SeNPs) remain insufficiently characterized. This study aimed to test the hypothesis that biosynthesized SeNPs inhibit S. mutans growth and biofilm formation through downregulation of the biofilm-associated gtfB gene.
Methods: SeNPs were biosynthesized using Artemisia scoparia extract and characterized for nanoscale morphology. Their antibacterial activity against *S. mutans* was assessed using standard in vitro susceptibility assays, while antibiofilm effects were evaluated using biofilm detection methods. The impact of SeNPs exposure on *gtfB* gene expression was analyzed by RT-PCR and compared with untreated controls.
Results: The biosynthesized SeNPs demonstrated significant antibacterial activity against S. mutans and induced a reduction in biofilm-associated phenotypic characteristics. Gene expression analysis revealed significant downregulation of *gtfB* expression in treated samples compared with untreated controls.
Conclusion: Within the limitations of an in vitro model, biosynthesized SeNPs demonstrated antibacterial and antibiofilm activity against *S. mutans*, likely mediated through inhibition of *gtfB* expression. These findings suggest that SeNPs may serve as a promising adjunctive strategy for controlling cariogenic biofilms. However, further in vivo studies and comparative evaluations with existing antimicrobial agents are required to establish clinical relevance.
Key Words: Selenium Nanoparticles, *Streptococcus Mutans*, Antimicrobial Effects, Biofilm Gene Expression

Received: 12 June 2026 | **Accepted:** 20 July 2026 | **ePublished:** Summer and Autumn 2026; Vol. 38, No. 3-4

Introduction

Dental caries is a biofilm-mediated, multifactorial disease and remains one of the most prevalent chronic conditions worldwide. Globally, it is estimated that 2.3 billion people suffer from caries of permanent teeth; this rate is more than 530 million for children (1). Beyond oral destruction, untreated dental caries has been associated with systemic complications, including cardiovascular disease, upper respiratory tract infections, and alveolar bone loss (2-5).

Dental caries is the irreversible tooth demineralization as a consequence of carbohydrates fermentation in the presence of acids produced by acidogenic bacteria in the oral cavity. These bacteria get attached to the tooth surface, as structures called dental biofilm (plaque). Oral biofilm is a three-dimensional structure, made up of bacteria, epithelial cells, and leucocytes, in a matrix of carbohydrates and minerals (6). A study used fluorescence in situ hybridization (FISH) and showed that coaggregation and adhesion between

Streptococcus spp. and *Actinomyces spp.* is the reason for initial biofilm formation (7). *Streptococcus spp*. are present in most individual's oral cavity and colonize at many oral sites (8). *Streptococcus mutans* plays an important role in the initiation and progression of dental caries. These bacteria directly ferment sucrose and other sugars and cause demineralization and tooth decay by producing lactic acid (7). Acid production and acid tolerance by making exopolysaccharides (EPS) are the most important virulence factors of the *S.mutans*. More than 90% of the biofilm matrix is composed of EPS. This matrix contributes to antimicrobial resistance by limiting the diffusion of agents, thereby preventing them from reaching the bacterial cells (9).

Therefore, there is an increasing interest in developing nanoscale systems to combat biofilm formation. Nanoparticles have high penetration power and strong antimicrobial activity. They exhibit efficient antibacterial activity due to their high surface-to-volume ratio (10).

Among metal-based nanoparticles, selenium nanoparticles (SeNPs) have attracted increasing attention due to their lower toxicity, higher biocompatibility, and greater physicochemical stability compared to other selenium forms. SeNPs have demonstrated a broad spectrum of biological activities, including antioxidant, anticancer, and antimicrobial effects (11, 12).

SeNPs can be synthesized through chemical, physical, or biological routes; however, green synthesis using plant extracts is particularly advantageous because it is cost-effective, is environmentally friendly, and does not require harsh conditions (13, 14). Plant-derived phytochemicals act as reducing and stabilizing agents, enabling the formation of biocompatible nanoparticles with enhanced biological activity (15).

The genus *Artemisia* is rich in bioactive secondary metabolites, including flavonoids and terpenoids, which are known for their metal-reducing capabilities (16, 17). These compounds facilitate nanoparticle biosynthesis while potentially imparting additional antimicrobial properties. Despite evidence supporting the utility of *Artemisia* species in green nanoparticle synthesis, their application in the biosynthesis of SeNPs targeting cariogenic biofilms remains insufficiently explored.

Given the global burden of dental caries, the increasing resistance of biofilms to conventional antimicrobials, and the lack of effective vaccines despite decades of research (18), novel antibiofilm agents are urgently needed. To date, limited studies have investigated the effects of SeNPs biosynthesized using *Artemisia* extracts on *S. mutans* biofilm formation.

Therefore, the aim of this study was to biosynthesize SeNPs using *Artemisia* extract and to evaluate their antibacterial and antibiofilm activities against *S. mutans*, with particular emphasis on their potential to overcome biofilm-associated resistance mechanisms**.**

Methods and Materials

Preparation of the Plant Extract

Artemisia scoparia was obtained from the Herbarium of the Iranian Biological Resources Center, Tehran, Iran (Voucher specimen No. IBRCP1328). Fresh aerial parts of the plant were washed thoroughly with distilled water several times and subsequently air-dried in the shade for one to two weeks.

The *Artemisia* extract was prepared using the Soxhlet extraction method. Specifically, 50 g of dried leaf powder was subjected to extraction with 500 mL of ethanol (96%) in a Soxhlet apparatus for 12 hours. The resulting solvent was then evaporated using a rotary evaporator (Rv10 digital, Germany). Finally, the extract was filtered through Whatman No. 1 filter paper (Whatman plc, Kent, UK) and stored at 4°C until further use.

Synthesis of SeNPs

For the biosynthesis of SeNPs, 20 mL of plant extract (5 mg/mL) was added to 20 mL of 40 mM sodium selenite solution (Merck, Germany). The mixture was stirred continuously for 5 minutes at room temperature under ambient pH conditions, without external adjustment. The reaction mixture was then left undisturbed until the development of an orange color, indicating the reduction of selenite ions to SeNPs.

The synthesized nanoparticles were subsequently collected by centrifugation at 13,000 rpm for 20 minutes, washed with distilled water, and dried at 75°C for 2 hours. Characterization by scanning electron microscopy (SEM) and transmission electron microscopy (TEM) confirmed that the drying process did not induce observable changes in

nanoparticle morphology or size distribution. All biosynthesis experiments were performed in triplicate to ensure reproducibility. Quantitative reaction yield was not calculated, as the primary objective of this study was green synthesis and biological evaluation, rather than optimization of production efficiency.

Characterization of SeNPs

Transmission Electron Microscopy

The surface morphology and size distribution of the biosynthesized nanoparticles were characterized using transmission electron microscopy (TEM). Imaging was performed with a Zeiss 100 kV microscope (Germany) operating at an accelerating voltage of 120 kV. Micrographs were captured at magnifications ranging from 20,000× to 200,000×, providing a point resolution of approximately 0.34 nm. To prepare specimens for analysis, a drop of the aqueous SeNP suspension was deposited onto a carbon-coated copper grid and allowed to air-dry at ambient temperature. Subsequent particle size analysis was conducted using ImageJ software (National Institutes of Health, USA).

Scanning Electron Microscopy

For scanning electron microscopy (SEM) analysis, an aqueous suspension of the biosynthesized SeNPs was prepared. The nanoparticles were subsequently mounted onto aluminum stubs with adhesive tape and sputter-coated with a thin layer of gold using an SBC12 sputter coater (KYKY). Imaging was performed with an XL30 scanning electron microscope (Philips, Netherlands) operating at 30 kV. Micrographs were captured at magnifications ranging from 1,000× to 100,000×, providing a spatial resolution of approximately 3.5 nm.

Antibacterial Study of SeNPs

The minimum inhibitory concentration (MIC) of SeNPs against *Streptococcus mutans* was determined using the broth microdilution method according to Clinical and Laboratory Standards Institute (CLSI) guidelines (2017). A serial two-fold dilution of SeNPs was prepared, yielding concentrations ranging from 3.125 to 100 µg/mL. Bacterial suspensions were adjusted to a 0.5 McFarland standard, corresponding to approximately 10^8 CFU/mL. For the assay, 5 µL of the bacterial suspension, 95 µL of Mueller-Hinton (MH) broth, and 100 µL of each SeNP dilution were loaded into the wells of sterile 96-well microtiter plates. Growth control wells (negative control for treatment) contained MH broth and bacterial suspension only, while chlorhexidine served as a positive control. The plates were sealed, shaken at 100 rpm for 60 seconds, and subsequently incubated at 37°C for 24 hours. All experiments were performed in triplicate across three independent runs. Following incubation, the MIC was defined as the lowest concentration of SeNPs that completely inhibited visible bacterial growth. Turbidity in control and experimental wells was recorded both before and after incubation to confirm MIC values.

Antibiofilm Study of SeNPs

The Congo Red Agar (CRA) test developed by Freeman et al. (19) was used as a qualitative phenotypic screening method to assess biofilm-associated characteristics rather than as a quantitative assay for biofilm biomass determination. For this method, a concentrated aqueous solution of Congo Red Stain (Merck, Germany) was prepared and autoclaved (121°C for 15 minutes). A mixture of brain heart infusion broth (Merck, Germany) 37 g/L, agar No. 1 (Merck, Germany) 10 g/L, and sucrose 50 g/L (Merck, Germany) was prepared and Congo Red (BDH Ltd) 0.8 g/L was added to the mixture. Then, the media were refrigerated. 100 µL of bacterial suspension in MH broth (0.5 McFarland) was mixed with 100 µL of different Sub-MIC concentrations of SeNPs (½ MIC, ¼ MIC, and concentrations ⅛ MIC = 1.5625 µg/mL) followed by incubation at 37 °C for 24 h. Afterward, the bacteria were inoculated into CRA medium and incubated at 37°C for another 24 h. Changes observed on CRA were interpreted qualitatively as alterations in biofilm-associated phenotypic characteristics. Quantitative biofilm inhibition was not assessed using this method. In this medium, biofilm-producing bacteria form black colonies with a dry crystalline appearance, whereas non-slime producers typically form pink colonies. *S. mutans* naturally produces biofilm and forms black colonies; therefore, the appearance of pink colonies following SeNP treatment was interpreted as an antibiofilm effect. This study acknowledges the limitations inherent to the qualitative CRA method, including its reliance on subjective visual assessment and its susceptibility to yielding false-positive or false-negative results. Therefore, the findings pertaining to biofilm-associated phenotypic changes were interpreted with appropriate caution.

Gene Expression (qRT-PCR)

Quantitative real-time PCR (qRT-PCR) was conducted to analyze the effect of SeNPs treatment on the expression of the virulence gene *gtfB* of *S. mutans*. A 100 µL aliquot of bacterial suspension in MH broth (0.5 McFarland) was added to 100 µL of different sub-MIC concentrations of SeNPs (½ MIC, ¼ MIC, and ⅛ MIC = 1.5625 µg/mL) and incubated at 37°C for 24 h. After incubation, RNA was isolated using RNX-PLUS (CinnaGen, Iran). Purified RNA was dissolved in diethyl pyrocarbonate-treated water and stored at −80°C until cDNA synthesis.

Complementary DNA (cDNA) was synthesized using the RevertAid™ First Strand cDNA Synthesis Kit (Fermentas, USA). DNase treatment was performed prior to reverse transcription to eliminate genomic DNA contamination. The reverse transcription reaction was carried out at 42°C for 60 min, followed by enzyme inactivation at 70°C for 10 min. The resulting cDNA samples were stored at −20°C until further analysis.

Real-time PCR was performed using the SYBR Green real-time RT-PCR method on an Exicycler™ 96 (Bioneer, Korea). The PCR conditions involved an initial denaturation at 95°C for 10 min, followed by 40 cycles of amplification, with each cycle consisting of denaturation at 95°C for 20 s and annealing and extension at 61°C for 40 s. The primer sequences are listed in Table 1. The 16S ribosomal RNA (rRNA) gene of *S. mutans* was used as the internal reference for normalization of *gtfB* expression due to its widespread application and reported stability in *Streptococcus mutans* under in vitro experimental conditions.

Primer	Sequence (5-3)	Size (bp)
gtfB-F	F AGCAATGCAGCCATCTACAAAT	153
gtfB-R	R ACGAACTTTGCCGTTATTGTCA	153
16SrRNA-F	GAGCGGCGGACGGGTGAGTA	110
16SrRNA-R	GGGCACATCTGATGGCATGA	110

Table 1. Primers used for gene investigation of *S. mutans* exposed to SeNPs

All reactions were performed in three biological replicates, each with three technical replicates. Relative gene expression levels were calculated using the ΔΔCt method, with untreated bacterial cultures serving as the calibrator. Data are presented as fold-change in *gtfB* expression relative to the control.

Statistical Analysis

Statistical analyses were performed using one-way analysis of variance (ANOVA) to evaluate differences in gene expression among the experimental groups. Following ANOVA, Tukey's honestly significant difference (HSD) post hoc test was applied for multiple comparisons between treatment groups and the control group.

All experiments were conducted in triplicate, and the data are presented as the mean ± standard deviation (SD). Statistical analyses were carried out using SPSS software (IBM Corp., Armonk, NY, USA). A p-value of less than 0.05 was considered to indicate statistical significance.

Results

Synthesis of SeNPs

A visible color change from colorless to orange, indicating the conversion of Na_2SeO_3 into SeNPs, was observed during the synthesis process and served as a preliminary qualitative indicator of nanoparticle formation (Figure 1).

Figure 1 presents representative images of (A) the *Artemisia scoparia* plant extract and (B) the reaction mixture following SeNP synthesis. These images are representative of typical observations obtained from experiments performed in triplicate.

(A) (B)

Figure 1. A: Preparing plant extract, B: SeNPs synthesis

Characterization of SeNPs

The particle size of the synthesized SeNPs was analyzed using transmission electron microscopy (TEM) (Figure 2a). Quantitative analysis of 529 individual particles revealed a mean diameter of 16.69 nm ± 18.40 nm (standard deviation) (Figure 2b).

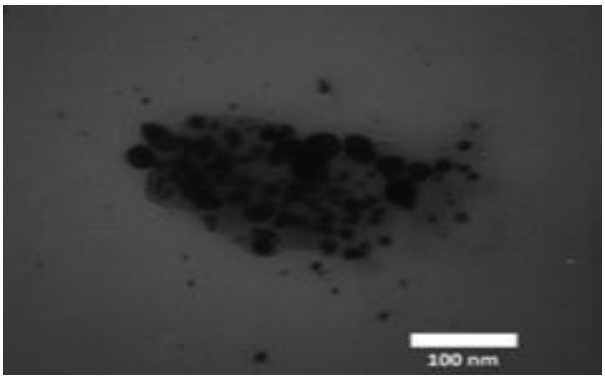

(A)

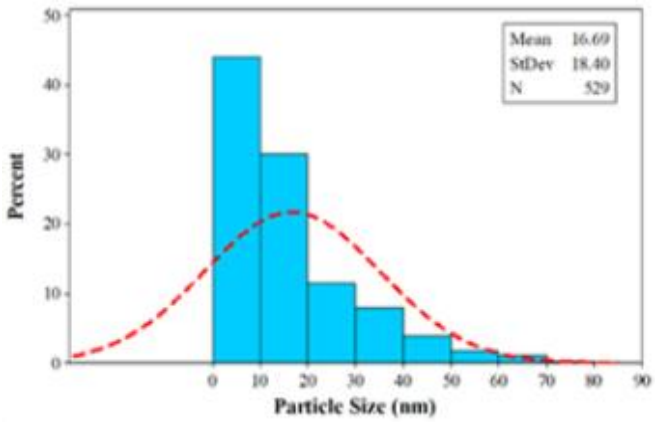

(B)

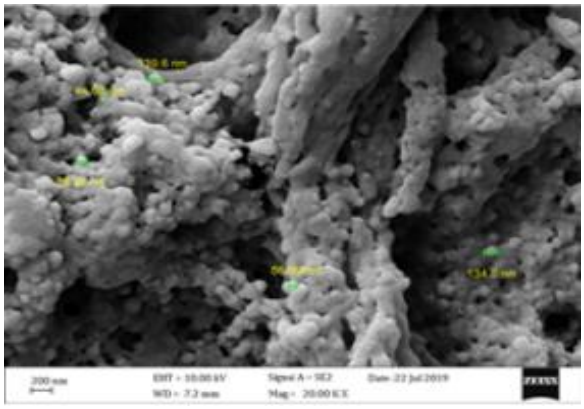

(C)

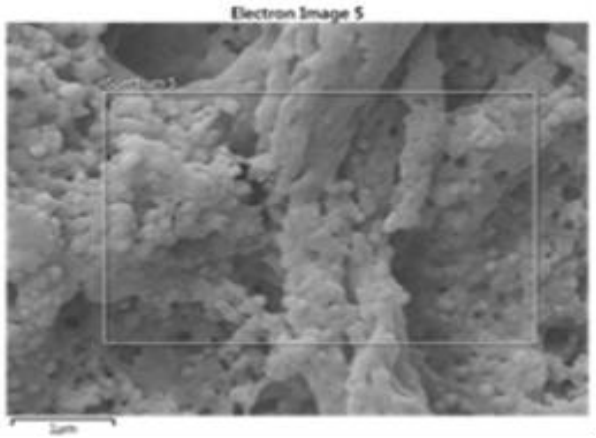

(D)

Figure 2. Characterization of SeNPs. **a:** Transmission electron microscopy image of SeNPs. **b:** Particle size ~16.69 nm. **c:** Scanning electron microscopy image of SeNPs. **d:** EDX results

Scanning electron microscopy (SEM) was employed to examine the surface morphology of the biosynthesized SeNPs (Figure 2c). Evaluation of the micrographs indicated that the nanoparticles were predominantly spherical, confirming a relatively uniform morphology.

Energy-dispersive X-ray spectroscopy (EDX) analysis was performed to determine the elemental composition of the nanoparticles. The resulting spectrum confirmed selenium as the major constituent, with an atomic percentage of 78.1%, indicating successful synthesis and high elemental purity of the SeNPs (Figure 2d).

Antibacterial evaluation of SeNPs

The antibacterial activity of the SeNPs against *Streptococcus mutans* was evaluated using the Mueller–Hinton broth microdilution method. SeNPs were tested at concentrations of 3.125, 6.25, 12.5, 25, 50, and 100 µg/mL. The MIC of SeNPs against *S. mutans* was determined to be 12.5 µg/mL. MIC assays were performed in triplicate, and the reported value represents the lowest concentration that consistently inhibited visible bacterial growth across all independent experiments. MIC determination was based on endpoint visual assessment of growth inhibition; optical density measurements and growth curve analyses were not performed.

For comparison, the antibacterial efficacy of SeNPs was benchmarked against chlorhexidine, which served as a positive control under identical experimental conditions. This comparative analysis demonstrated that SeNPs exhibited notable antibacterial activity, although the MIC value was higher than that observed for the standard antimicrobial agent.

The antibacterial activity of the SeNPs against *Streptococcus mutans* was evaluated using the Mueller–Hinton broth microdilution method. SeNPs were tested at concentrations of 3.125, 6.25, 12.5, 25, 50, and 100 µg/mL. The minimum inhibitory concentration (MIC) of SeNPs against *S. mutans* was determined to be 12.5 µg/mL. MIC assays were performed in triplicate, and the reported value represents the lowest concentration that consistently inhibited visible bacterial growth across all independent experiments. MIC determination was based on endpoint visual assessment of growth inhibition; optical density measurements and growth curve analyses were not performed.

For comparison, the antibacterial efficacy of SeNPs was benchmarked against chlorhexidine, which served as a positive control under identical experimental conditions. This comparative analysis demonstrated that SeNPs exhibited notable antibacterial activity, although the MIC value was higher than that observed for the standard antimicrobial agent.

Antibiofilm Assessment of SeNPs

To evaluate the antibiofilm activity of SeNPs against *Streptococcus mutans*, the CRA test was employed. Changes observed on CRA were interpreted qualitatively as indications of alterations in biofilm-associated phenotypic characteristics. Quantitative assessment of biofilm inhibition was not performed using this method. Figure 3 presents representative images of the qualitative CRA phenotypic observations. As shown in Fig. 3, bacteria treated with sub-MIC concentrations of SeNPs did not produce black colonies on CRA medium, suggesting a modification in biofilm-associated phenotypic characteristics following SeNP treatment. CRA results were evaluated qualitatively, and therefore, statistical analysis was not applicable to this assay. The inherent limitations of the CRA method are acknowledged, including its susceptibility to subjective interpretation and the potential for false-positive or false-negative results. Accordingly, these findings were interpreted with caution.

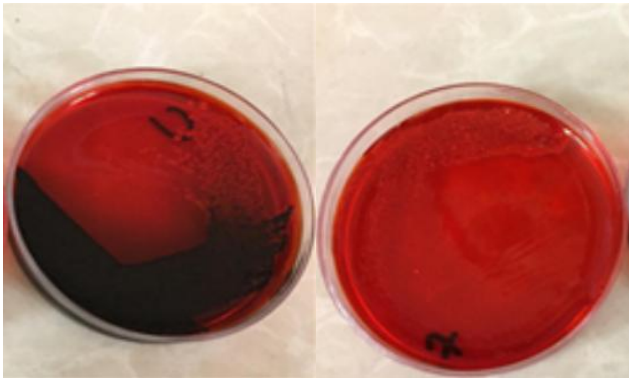

(A) (B)

Figure 3. Phenotypic study of anti-biofilm effects. a: *S.mutans* in CRA medium before treatment with SeNPs. b: *S. mutans* after treatment with SeNPs formed pink colonies (lack of black clonies formation)

Expression of *gtfB* Gene by Real-Time PCR

Quantitative real-time PCR (qRT-PCR) was performed to assess the effect of SeNPs on the expression of the virulence gene *gtfB* in *Streptococcus mutans*. Relative gene expression levels were calculated using the ΔΔCt method, with the 16S rRNA gene serving as the internal reference control. Treatment with SeNPs at ½ MIC and ¼ MIC concentrations resulted in a significant downregulation of *gtfB* expression, as evidenced by reduced fold-change values compared with the untreated control ($p < 0.001$). In contrast, exposure to ⅛ MIC SeNPs did not produce a statistically significant change in *gtfB* expression relative to the control group ($p > 0.05$), indicating a concentration-dependent effect. All experiments were performed in triplicate, and results are presented as mean fold change ± standard deviation (SD), allowing for assessment of variability across replicates. The fold-change values for both the target (*gtfB*) and reference (16S rRNA) genes are summarized in Table 2. Amplification plots and melt curve analyses confirming the specificity of the qRT-PCR reactions are presented in Fig. 5, while relative expression levels are illustrated in Figure 4.

Quantitative real-time PCR (qRT-PCR) was performed to assess the effect of SeNPs on the

expression of the virulence gene *gtfB* in *Streptococcus mutans*. Relative gene expression levels were calculated using the ΔΔCt method, with the 16S rRNA gene serving as the internal reference control.

Concentration of SeNPs	Fold change values	
	16S rRNA gene	*gtfB* gene
½ MIC	0.98±0.08	0.66±0.02
¼ MIC	0.98±0.07	0.41±0.08
⅛ MIC	0.98±0.05	0.92±0.07

Table 2. Relative fold change in (*gtfB*) and (16S rRNA) gene expression of *S. mutans* treated with different concentrations of selenium nanoparticles

Treatment with SeNPs at ½ MIC and ¼ MIC concentrations resulted in a significant downregulation of *gtfB* expression, as evidenced by reduced fold-change values compared with the untreated control ($p < 0.001$). In contrast, exposure to ⅛ MIC SeNPs did not produce a statistically significant change in *gtfB* expression relative to the control group ($p > 0.05$), indicating a concentration-dependent effect.

All experiments were performed in triplicate, and results are presented as mean fold change ± standard deviation (SD), allowing for assessment of variability across replicates. The fold-change values for both the target (*gtfB*) and reference (16S rRNA) genes are summarized in Table 2. Amplification plots and melt curve analyses confirming the specificity of the qRT-PCR reactions are presented in Fig. 5, while relative expression levels are illustrated in Figure 4.

Quantitative real-time PCR (qRT-PCR) was performed to assess the effect of SeNPs on the expression of the virulence gene *gtfB* in *Streptococcus mutans*. Relative gene expression levels were calculated using the ΔΔCt method, with the 16S rRNA gene serving as the internal reference control. Treatment with SeNPs at ½ MIC and ¼ MIC concentrations resulted in a significant downregulation of *gtfB* expression, as evidenced by reduced fold-change values compared with the untreated control (*p* < 0.001). In contrast, exposure to ⅛ MIC SeNPs did not produce a statistically significant change in *gtfB* expression relative to the control group ($p > 0.05$), indicating a concentration-dependent effect. All experiments were performed in triplicate, and results are presented as mean fold change ± standard deviation (SD), allowing for assessment of variability across replicates. The fold-change values for both the target (*gtfB*) and reference (16S rRNA) genes are summarized in Table 2. Amplification plots and melt curve analyses confirming the specificity of the qRT-PCR reactions are presented in Fig. 5, while relative expression levels are illustrated in Figure 4.

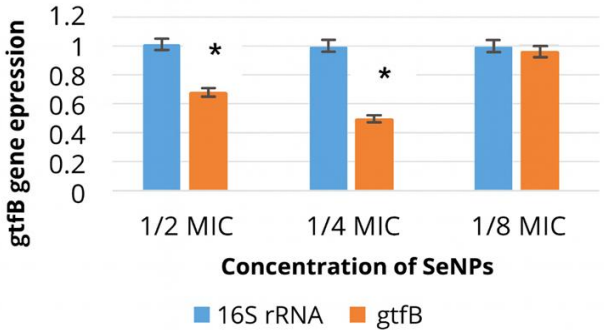

Figure 4. Expression of *gtfB* gene in S.mutans in response to treatment with sub-MIC concentration of SeNPs. The data presented were generated from at least three independent sets of experiments (data=mean±SD). Statistical significance as compared with the untreated control ($p<0.05$) denoted by an asterisk (*) *(Colors must be printed)*

Discussion

Dental biofilms are largely composed of exopolysaccharides, which restrict the penetration of conventional antimicrobial agents (7). Nanoscale antimicrobial systems, owing to their small size and high surface-area-to-volume ratio, can potentially overcome this limitation by penetrating the biofilm matrix and interacting more effectively with bacterial cells. In this context, SeNPs may exert antibacterial effects through multiple mechanisms, including disruption of bacterial cell membranes, interference with metabolic pathways, and modulation of virulence gene expression. Although the precise molecular interactions were not examined in the present study, the observed suppression of *gtfB* expression suggests that SeNPs

may impair biofilm development at the genetic level, in addition to inhibiting planktonic bacterial growth.

In the current study, SeNPs were synthesized using a green, facile, and eco-friendly approach with *Artemisia scoparia* extract serving as a bio-reductant, yielding spherical nanoparticles with a mean size of 16.69 nm. The presence of phenols, flavonoids, terpenoids, and other reducing agents in *Artemisia* species has been previously documented, supporting their suitability for nanoparticle synthesis. Similar successful applications of *Artemisia* extracts in nanoparticle biosynthesis have been reported by Salehi et al. (17) and Kaviani et al. (20). The relatively small particle size obtained here may be attributed to the phytochemical composition of the extract, which can influence nucleation and stabilization during nanoparticle formation.

Other studies have employed different plant extracts for SeNP synthesis. Yazhiniprabha and Vaseeharan (21) utilized an aqueous berry extract of *Murraya koenigii* and obtained spherical nanoparticles with a larger size range (50–150 nm), substantially larger than the SeNPs synthesized in the present work. Such differences in particle size, synthesis route, and phytochemical capping agents are known to significantly influence antimicrobial potency and minimum inhibitory concentration (MIC) values. Size is a critical determinant of the biological activity of nanoparticles, as smaller particles possess a higher surface-to-volume ratio, enhanced surface reactivity, and improved interaction with bacterial cell membranes, which can result in lower MIC values and stronger antibacterial effects (11). Therefore, the comparatively lower MIC observed here may be attributed to the smaller particle size and the *Artemisia*-mediated biosynthesis process, which likely affects surface chemistry and bioactivity.

In this study, SeNPs were evaluated against *Streptococcus mutans*, the primary etiological agent of dental caries. Unlike previous investigations that focused predominantly on growth inhibition, this work provides both phenotypic and molecular-level evidence of antibiofilm activity. Bacterial growth was significantly inhibited, and the MIC of SeNPs against *S. mutans* was determined to be 12.5 µg/mL, a value lower than those reported in earlier studies. Importantly, this is one of the first studies to demonstrate *gtfB* gene suppression using real-time PCR, thereby linking SeNP exposure to disruption of exopolysaccharide synthesis at the molecular level.

The enhanced antibacterial efficacy observed in the present study may be attributed to the *Artemisia*-based biosynthesis approach, which influences nanoparticle size, shape, and surface chemistry through plant-derived capping agents. Comparative studies support this interpretation. Yazhiniprabha and Vaseeharan (21) reported an MIC of 40 µg/mL for SeNPs synthesized with *M. koenigii* extract, while Shubharani et al. (22) reported a markedly higher MIC of 500 µg/mL for oval-shaped SeNPs. These differences underscore the critical role of nanoparticle size, morphology, and synthesis method in determining antimicrobial potency. Smaller nanoparticles provide a higher surface-to-volume ratio and enhanced interaction with bacterial cells, leading to greater antibacterial activity (11). Accordingly, the lower MIC observed in the current study highlights the added value of *Artemisia*-mediated SeNP synthesis combined with molecular validation of antibiofilm mechanisms.

Glucosyltransferase genes, particularly *gtfB*, play a pivotal role in the synthesis of insoluble glucans that facilitate *S. mutans* adherence and biofilm maturation. Inhibiting *gtfB* expression can disrupt colonization and plaque formation (23). The present study demonstrated a significant reduction in *gtfB* expression at sub-inhibitory concentrations (½ MIC and ¼ MIC) of SeNPs, indicating that these nanoparticles can attenuate virulence without necessarily causing complete bacterial eradication. This molecular-level evidence represents a key contribution of the study. While previous work, such as that by Haris and Khan (24), has shown antibiofilm effects of SeNPs—particularly in combination with photodynamic therapy—the current study provides direct evidence of virulence gene suppression using real-time PCR in a biosynthesized SeNP system.

Despite these promising findings, several limitations should be acknowledged. This study was conducted entirely in vitro, and therefore the results may not fully reflect the complex conditions of the oral cavity. The Congo red agar method employed for biofilm assessment is qualitative and is not considered a gold standard; more robust quantitative assays, such

as crystal violet staining or microtiter plate biofilm assays, were not performed and should be incorporated in future investigations to validate and quantify antibiofilm activity. Additionally, cytotoxicity, biocompatibility, dose–response relationships, long-term nanoparticle stability, and potential systemic effects were not evaluated. These factors are critical for assessing the safety and translational potential of SeNPs for oral applications. Within these limitations, the findings suggest that *Artemisia scoparia*–mediated SeNPs exhibit notable antibacterial and antibiofilm activity against *S. mutans*, supported by both phenotypic and molecular evidence. While these results indicate potential for future application in caries prevention strategies, further in vivo and clinical studies are necessary to evaluate safety, efficacy, and feasibility before incorporation into oral healthcare products such as mouthwashes or toothpastes.

Conclusion

Artemisia scoparia extract was successfully employed in the green synthesis of SeNPs, demonstrating its suitability as a capping and stabilizing agent. The biosynthesized SeNPs exhibited appropriate physicochemical characteristics along with notable antibacterial and antibiofilm activity against S. mutans under in vitro conditions. These findings suggest that SeNPs synthesized using A. scoparia have potential as an adjunct strategy for controlling dental cariogenic bacteria. However, further studies, including cytotoxicity assessment, formulation optimization, and evaluation in relevant animal models, are required before they can be considered for clinical applications.

Declarations

Ethical Approval and Consent to Participate

The present study did not involve human subjects, human material, or human data. Therefore, consent to participate is not applicable. Likewise, no animal experiments or ethically regulated biological samples were used, so formal ethical approval was not required.

Availability of Data and Materials

All data generated or analyzed during this study are included in this published article. Raw data and supplementary materials are available from the corresponding author upon reasonable request. No human or animal subjects were involved, and no third-party datasets requiring special permissions were used.

Competing Interests

The authors declare that they have no known competing financial interests or personal relationships that could have appeared to influence the work reported in this paper.

Funding

This research did not receive any specific grant from funding agencies in the public, commercial, or not-for-profit sectors. No financial support was provided for the design, data collection, analysis, interpretation, or writing of this manuscript.

Authors' Contributions

Niyousha Noorullahi (N.N.) contributed to investigation and writing—original draft preparation. Farid Abbasi (F.A.) and Ronak Bakhtiari (R.B.) contributed equally to formal analysis and validation. Aliyeh Sehatpour (A.S.) contributed to supervision, project administration, and resources. All authors read and approved the final manuscript.

Declaration of Generative Artificial Intelligence (AI) Utilization

The authors hereby confirm that artificial intelligence (AI) tools were utilized exclusively for grammar improvement and language editing to enhance the readability of this manuscript. No AI or AI-assisted technologies were employed in the research process itself, including study design, data collection, data analysis, interpretation of findings, or generation of figures and tables. All scientific content, intellectual contributions, and conclusions are the original work of the authors. Following the use of AI for language polishing, the authors conducted a thorough review and revision of the text and take full responsibility for the final version of the manuscript.

Acknowledgments

The authors would like to acknowledge the Department of Pathobiology, School of Public Health, Tehran University of Medical Sciences, for their support and assistance in this study.

References

1. Peres MA, Macpherson LM, Weyant RJ, Daly B, Venturelli R, Mathur MR, et al. Oral diseases: a global public health challenge. The Lancet. 2019;394(10194):249-60.

2. Zhou Y, Jiang S, Li KY, Lo ECM, Gao X. Association between oral health and upper respiratory tract infection among children. International Dental Journal. 2018; 68(2): 122-8.

3. Gao L, Xu T, Huang G, Jiang S, Gu Y, Chen F. Oral microbiomes: more and more importance in oral cavity and whole body. Protein & cell. 2018;9(5):488-500.

4. Fernandes T, Bhavsar C, Sawarkar S, D'souza A. Current and novel approaches for control of dental biofilm. International journal of pharmaceutics. 2018;536(1):199-210.

5. Hardan L, Matta A, Bourgi R, Cuevas-Suarez CE, Devoto W, Zarow M, et al. Association between Dental and Cardiovascular diseases: a systematic review. Reviews in Cardiovascular Medicine. 2023;24(6):159.

6. Hajishengallis G, Lamont RJ, Koo H. Oral polymicrobial communities: Assembly, function, and impact on diseases. Cell host & microbe. 2023;31(4):528-38.

7. Valm AM. The structure of dental plaque microbial communities in the transition from health to dental caries and periodontal disease. Journal of molecular biology. 2019;431(16):2957-69.

8. Paster BJ, Olsen I, Aas JA, Dewhirst FE. The breadth of bacterial diversity in the human periodontal pocket and other oral sites. Periodontology 2000. 2006; 42 (1).

9. Afrasiabi S, Partoazar A. Targeting bacterial biofilm-related genes with nanoparticle-based strategies. Frontiers in Microbiology. 2024;15:1387114.

10. Rosli NA, Teow YH, Mahmoudi E. Current approaches for the exploration of antimicrobial activities of nanoparticles. Science and Technology of Advanced Materials. 2021;22(1):885-907.

11. Hosnedlova B, Kepinska M, Skalickova S, Fernandez C, Ruttkay-Nedecky B, Peng Q, et al. Nano-selenium and its nanomedicine applications: a critical review. International journal of nanomedicine. 2018:2107-28.

12. Cremonini E, Zonaro E, Donini M, Lampis S, Boaretti M, Dusi S, et al. Biogenic selenium nanoparticles: c haracterization, antimicrobial activity and effects on human dendritic cells and fibroblasts. Microbial biotechnology. 2016;9(6):758-71.

13. Bhiri N, Masquelez N, Nasri M, Nasri R, Hajji M, Li S. Synthesis, Characterization, and Stability Study of Selenium Nanoparticles Coated with Purified Polysaccharides from Ononis natrix. Nanomaterials. 2025; 15(6):435.

14. Gudkov SV, Gao M, Simakin AV, Baryshev AS, Pobedonostsev RV, Baimler IV, et al. Laser ablation-generated crystalline selenium nanoparticles prevent damage of DNA and proteins induced by reactive oxygen species and protect mice against injuries caused by radiation-induced oxidative stress. Materials. 2023; 16 (14):5164.

15. Hussain I, Singh N, Singh A, Singh H, Singh S. Green synthesis of nanoparticles and its potential application. Biotechnology letters. 2016;38(4):545-60.

16. Nguyen PT, Nguyen MT, Quach LT, Nguyen LL, Quyen DV. Antibiofilm activity of alpha-mangostin loaded nanoparticles against Streptococcus mutans. Asian Pacific Journal of Tropical Biomedicine. 2020;10(7):325-32.

17. Salehi S, Shandiz SAS, Ghanbar F, Darvish MR, Ardestani MS, Mirzaie A, et al. Phytosynthesis of silver nanoparticles using Artemisia marschalliana Sprengel aerial part extract and assessment of their antioxidant, anticancer, and antibacterial properties. International journal of nanomedicine. 2016:1835-46.

18. Patel M. Dental caries vaccine: are we there yet? Letters in applied microbiology. 2020;70(1):2-12.

19. Freeman D, Falkiner F, Keane C. New method for detecting slime production by coagulase negative staphylococci. Journal of clinical pathology. 1989;42(8): 872-4.

20. Kaviani N, Osfoori M. Biological Preparation of Silver Nanoparticles Using Artemisia â sieberi. Modares Journal of Biotechnology. 2025;9(1):23-7.

21. Yazhiniprabha M, Vaseeharan B. In vitro and in vivo toxicity assessment of selenium nanoparticles with significant larvicidal and bacteriostatic properties. Materials Science and Engineering: C. 2019;103:109763.

22. Shubharani R, Mahesh M, Yogananda Murthy V. Biosynthesis and characterization, antioxidant and antimicrobial activities of selenium nanoparticles from ethanol extract of Bee Propolis. J Nanomed Nanotechnol. 2019;10(2).

23. Kulshrestha S, Khan S, Hasan S, Khan ME, Misba L, Khan AU. Calcium fluoride nanoparticles induced suppression of Streptococcus mutans biofilm: an in vitro and in vivo approach. Applied microbiology and biotechnology. 2016;100(4):1901-14.

24. Haris Z, Khan AU. Selenium nanoparticle enhanced photodynamic therapy against biofilm forming streptococcus mutans. International Journal of Life Sciences Scientific Research. 2017;3:1287-94.